引用格式：ZHOU Yuxia, Aiziheerjiang Abulikemu, Dana Jiashaner, et al. High Energy, High Beam Quality Idler-resonant mid-infrared Optical Parametric Oscillator Based on $KTiOAsO_4$[J]. Acta Photonica Sinica, 2023, 52(2):0214001
周玉霞,艾孜合尔江·阿布力克木,达娜·加山尔,等. 基于闲频光谐振的中红外高能量、高光束质量$KTiOAsO_4$光学参量振荡器[J].光子学报,2023,52(2):0214001

基于闲频光谐振的中红外高能量、高光束质量 $KTiOAsO_4$光学参量振荡器

周玉霞,艾孜合尔江·阿布力克木,达娜·加山尔,塔西买提·玉苏甫
(新疆师范大学 物理与电子工程学院 新疆发光矿物与光功能材料研究重点实验室, 乌鲁木齐 830054)

摘 要:基于砷酸钛氧钾(KTA)晶体优良的非线性光学特性,研究了由1 μm Nd:YAG纳秒脉冲调Q激光器泵浦的高能量、高光束质量闲频光单谐振光参量振荡器。选取合适镀膜参数的腔镜、优化腔型设计,建立了一个稳定紧凑的半球形对称闲频光单谐振腔,实现了高能量、高光束质量的近-中红外激光输出。在输入泵浦光的(1.064 μm)最大能量为20.2 mJ时,输出信号光(1.535 μm)和闲频光(3.468 μm)的最大能量分别为2.91 mJ和1.13 mJ,对应信号光和闲频光的斜效率分别为20.9%和8.1%。闲频光单谐振的光参量振荡器具有更大的衍射损耗和光束发散角,可以极大的限制输出光束的光谱带宽、提高谐振闲频光的光束质量等优势,测量了输出中红外闲频光在两个正交方向上的光束质量因子分别为$M_x^2 \approx 1.1$, $M_y^2 \approx 1.1$。

关键词:非线性光学;闲频光谐振;光参量振荡器;光束质量;砷酸钛氧钾
中图分类号:O437.4 **文献标识码**:A **doi**:10.3788/gzxb20235202.0214001

0 引言

1.5~1.6 μm波段是重要的人眼安全和大气窗口波段,该波段的光束进入人眼时先被眼球表面吸收,不会到达视网膜,被广泛应用于激光测距、雷达、遥感、通信等多个领域[1-2]。其中1.54 μm波长是人眼安全的一个奇点,该波长的激光器在国防安全等要求严苛的领域具有极大的应用需求[3-5]。3~5 μm波段是重要的大气红外窗口波段,涵盖了大量CH_2、NO_2等工业污染气体的分子振动吸收峰,许多痕量气体分子在该波段具有非常强的吸收特性和基本的振动带,对于浓度比较低的微量气体元素,可以借助该波段的激光来准确检测分子含量和浓度[6-7]。因此,中红外激光在环境监测、痕量气体追踪、分子光谱学、有机材料加工等领域有着非常重要的应用[8-9]。为满足上述激光在实际生活中的重要应用,国内外多位研究者为此做出极大努力。非线性频率转换技术作为一种非常紧凑高效的频率拓展技术,可以将固体激光器输出的单一波长通过非线性晶体进行倍频(Second Harmonic Generation, SHG)[10]、和频(Sum Frequency Generation, SFG)[11]、光参量放大(Optical parametric Amplification, OPA)[12]、光参量振荡(Optical Parametric Oscillator, OPO)[13]、受激拉曼散射(Stimulated Raman Scattering, SRS)[14]等方式进行转换,是产生多波长、高能量、高光束质量近-中红外激光源的主要方式之一。

非临界相位匹配(Non-Critical Phase Matching, NCPM)的砷酸钛氧钾($KTiOAsO_4$, KTA)($\theta=90°$, $\varphi=0°$)晶体由于具有较大的非线性系数($d_{24}=3.43$ pm/V)和接收角,在非线性频率转换过程中不具有任何走离效应等特性而在研究中广受关注[15]。其极低的温度敏感性和高的损伤阈值(600 MW/cm^2)使得KTA

基金项目:国家自然科学基金(No. 11664041),新疆维吾尔自治区自然科学基金(No. 2021D01A114),新疆矿物发光材料及其微结构实验室(No. KWFG202202)
第一作者:周玉霞, 1275387358@qq.com
通讯作者:塔西买提·玉苏甫, taxmamat_84@sina.com
收稿日期:2022-08-13;**录用日期**:2022-10-20

晶体可以在高功率激光泵浦下有效运行[16-17]，相对于掺杂MgO周期性铌酸锂（MgO:PPLN）晶体，满足Ⅱ类非临界相位匹配（NCPM）的KTA晶体没有走离效应，并且输出光的光谱带宽窄，光束单色性非常好，是产生近-中红外高能量、高光束质量激光的极佳选择。目前，通过光参量振荡技术产生近-中红外激光的方法逐渐成熟，在实验中已经可以实现较宽波长调谐范围、输出能量和转换效率比较高的近-中红外激光输出[18-19]，但输出光的光束质量仍有待进一步提高。双谐振光参量振荡器起振阈值低，但稳定性较差，而单谐振光参量振荡器稳定性较好，所以中红外激光通常使用单谐振腔型产生。相对于闲频光单谐振的光参量振荡器，信号光单谐振光参量振荡器在实验中具有起振阈值低，输出能量高等优点，但由于产生的闲频光没有谐振、其模式未受到任何腔镜限制就直接输出腔外，导致输出的中红外激光光束质量较差。高光束质量的中红外激光源在超分辨率分子吸收光谱和超越衍射极限的红外吸收显微镜等方面具有非常重要的应用。为了提高输出中红外激光源的光束质量，多位研究者通过闲频光谐振的光参量振荡器来提高中红外激光的光束质量。TIIHONEN M团队在研究基于非共线周期性极化KTP-OPO的信号光谐振与闲频光谐振输出光谱及空间特性差异时，发现闲频光谐振的光参量振荡器具有更大的衍射损耗和角度色散，其输出谐振光的光束质量不仅得到显著的提升，而且光谱带宽也缩至近两倍小[20]。山东大学BAI Fen团队通过腔内泵浦闲频光谐振的KTA-OPO实现了光束质量因子为1.2的中红外激光输出，其总的功率转换效率为5.4%[21]。2018年HE Yang团队通过优化基于闲频光单谐振的MgO:PPLN-OPO的腔型设计，进一步提高了输出中红外光束的转换效率（>14%）和光束质量（$M_x^2\approx1.57$, $M_y^2\approx1.49$）[22]。自纳秒级闲频光单谐振光参量振荡器被证明以后，PARSA S团队提出光纤泵浦皮秒光参量振荡器技术，利用同步泵浦MgO:PPLN闲频光谐振腔，在波长调谐范围内得到了平均光束质量因子分别为$M^2<1.8$, $M^2<1.4$的闲频光（4 028～2 198 nm）和信号光（1 446～2 062 nm）[23]；NANDY B团队通过同步泵浦闲频光单谐振的皮秒光参量振荡器得到$M^2<2.3$的近红外激光输出[24]。可见，闲频光单谐振的光参量振荡器可以有效提高输出中红外激光的光束质量。最近，孟军等结合非临界相位匹配晶体KTA和基于高斯反射晶体的不稳定谐振腔体来有效提高输出近-中红外激光的光束质量，输出中红外闲频光在两个正交方向上的光束质量因子为$M_x^2=11.2$, $M_y^2=11.5$。相较于稳定谐振腔，非稳腔可以较好的提高输出光的光束质量[25]。

本文基于闲频光单谐振的光参量振荡器，利用腔外泵浦KTA-OPO技术，在中红外波段获得光束质量接近衍射极限的中红外激光（$M_x^2\approx1.1$, $M_y^2\approx1.1$）。通过选取合适镀膜参数的闲频光单谐振腔镜、优化腔型设计，极大的提高了近-中红外激光的输出能量。在泵浦光最大能量为20.2 mJ时，输出信号光（1.535 μm）和闲频光（3.468 μm）的最大能量可达2.91 mJ和1.13 mJ，对应斜效率分别为20.9%和8.1%。相对于之前研究者的相关报道，不仅提高了输出中红外激光源的光束质量，而且在近-中红外激光的输出能量中也有了很大的进步。

1 实验设置

基于闲频光单谐振的高能量、高光束质量的KTA-OPO的实验装置如图1所示。采用波长为1 μm的传统纳秒闪光灯调Q Nd:YAG固体激光器（Lotis LS-2136, pulse duration:25 ns; Pulse Repetition Frequency (PRF):50 Hz; wavelength:1 064 nm）为泵浦源，其输出光束具有近高斯空间分布。反向隔离器（Isolator）被用来防止反射光过强而损伤激光器。利用焦距$f=750$ mm的聚焦透镜（Lens）将泵浦光聚焦为1 mm光斑输

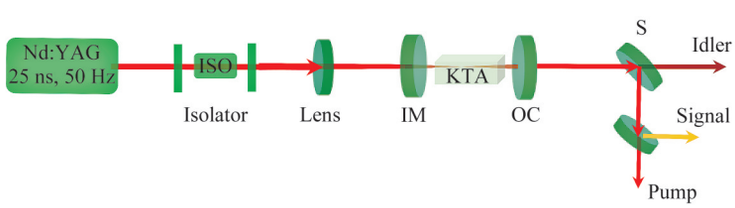

Nd:YAG is a pump laser; Faraday rotator used as an isolator; Lens is a focusing lens (f=750 mm);
IM and OC are the input mirror and output coupler; S is the Germanium filter

图1 高能量、高光束质量的KTA-OPO的实验装置

Fig.1 Schematic diagram of the experimental setup for the high-energy and high beam quality KTA-OPO

入到KTA晶体中。非线性介质KTA（$\theta=90°$，$\varphi=0°$）的规格为$5\times5\times30$ mm^3，满足Ⅱ类非临界相位匹配（NCPM），两端面镀有对泵浦光（1.064 μm）、信号光（1.535 μm）和闲频光（3.468 μm）的增透薄膜，使得泵浦光、信号光和闲频光在非线性晶体中具有最高的非线性增益和最小的能量损耗。闲频光单谐振光参量振荡器的腔型设计为稳定半对称腔，输入镜IM（$R=500$ mm）对泵浦光增透，对信号光（1.4～1.6 μm）和闲频光（3～4 μm）高反射。输出耦合镜OC采用对泵浦光和信号光高透射，对闲频光具有约80%反射率的平面镜，谐振腔总腔长固定为35 mm，建立了一个稳定紧凑的闲频光单谐振半球形对称腔。S滤波片对1.9 μm以下的短波长高反射、对3～5 μm的中红外光波透射率高达95%以上，可以有效保证泵浦光和信号光被反射，而闲频光被提取出来。利用上述实验仪器，搭建稳定紧凑的闲频光单谐振腔，输出高光束质量、高能量的中红外闲频光。

2 分析与讨论

采用常规的电荷耦合照相机（CCD）和高性能热释电相机（Spiricon Pyrocam Ⅲ，spatial resolution：75 mm）分别测量了泵浦光、信号光和闲频光的空间分布。如图2所示，泵浦光的空间强度分布（a）与输出的信号光（b）和闲频光（c）的空间强度分布图样完全相似，均为近高斯空间分布，而且输出激光的空间强度分布非常均匀。相对于信号光单谐振，由于闲频光具有更大的发散角，在谐振过程中容易产生衍射损耗，故闲频光单谐振的光参量振荡器具有较大的起振阈值和光束能量损耗，在实验过程中对腔镜镀膜的精度参数和光参量振荡器的腔型设计均具有很高的要求[21]。为了提高输出近-中红外激光的能量，本实验选择曲率半径为500 mm的凹面输入镜和平面输出镜来建立半球形对称稳定腔，这样的腔型设计可以有效限制谐振闲频光的模式尺寸。当谐振闲频光被曲率半径为500 mm的凹面输入镜反射到KTA晶体时，其模式尺寸缩小到与泵浦光相近，极大的增加了泵浦光与谐振闲频光在晶体内的模式耦合，进而提高了输出激光的能量和转换效率。

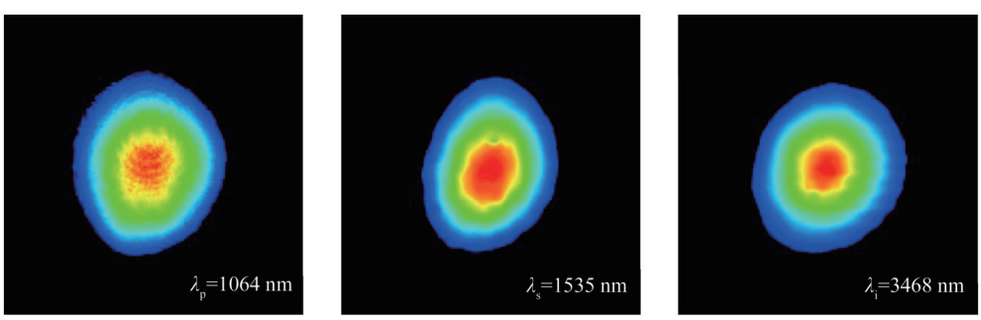

图2 泵浦光、信号光和闲频光的空间强度分布

Fig.2 Spatial intensity profile of pump beam, signal beam and idler beam

闲频光单谐振的光参量振荡器由于具有更大的衍射损耗和角度色散，进而限制了输出光束的光谱带宽，使得输出的中红外闲频光具有更窄的光谱带宽和更高的光束质量[20]。基于上述原理及实验数据，利用刀口法测得输出中红外闲频光在两个正交方向上的光束质量分别为$M_x^2\approx1.1$，$M_y^2\approx1.1$（图3）。另外，使用高性能扫描单色仪（SpectraPro HRS-500，300 line/mm，孔径尺寸50 μm，光谱分辨率0.3～0.4 nm，波长范围为1 000～5 000 nm）测量了输出近-中红外信号光和闲频光的激光光谱（图4）。可以发现，中心波长为1 535 nm和3 468 nm的近-中红外激光的半高宽分别为$\Delta\lambda_s\approx0.36$ nm，$\Delta\lambda_i\approx0.71$ nm，相较于信号光单谐振光参量振荡器所得的中红外闲频光光谱带宽（$\Delta\lambda_i\approx1.7$ nm）[13]，光谱带宽被极大的窄化。

通过上述实验设计，得到输出信号光和闲频光的能量与泵浦能量之间的函数关系，如图5所示。在泵浦光的最大泵浦能量为20.2 mJ时，输出信号光的最大能量是2.9 mJ、闲频光的最大能量为1.1 mJ，对应的信号光和闲频光的斜效率分别为20.9%和8.1%，本文测量了信号光和闲频光的输出能量稳定性，在12 h内的能量稳定性均小于2% rms。可以发现，相对于信号光单谐振的光参量振荡器，闲频光单谐振的光参量振荡器具有更高的起振阈值，对实验光路的设计也具有更高的要求[26]。在谐振腔的设计中选择高精度镀膜参数的腔镜，合理设计谐振腔型有望更进一步提高输出激光的能量和转换效率，减小闲频光在腔内谐振时的损耗，进而降低闲频光单谐振光参量振荡器的起振阈值。

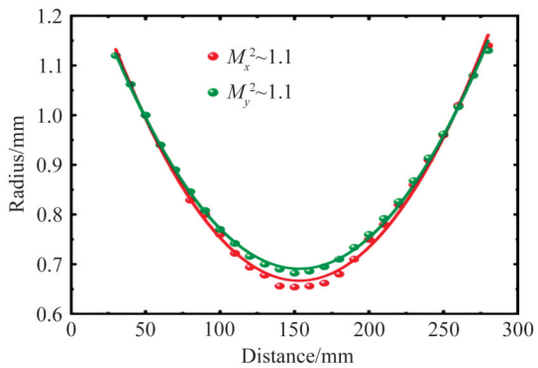

图3 中红外闲频光在两个正交方向上的光束质量因子(M^2)

Fig.3 The beam quality factors (M^2) of the mid-infrared idler wave in tow orthogonal directions were measured

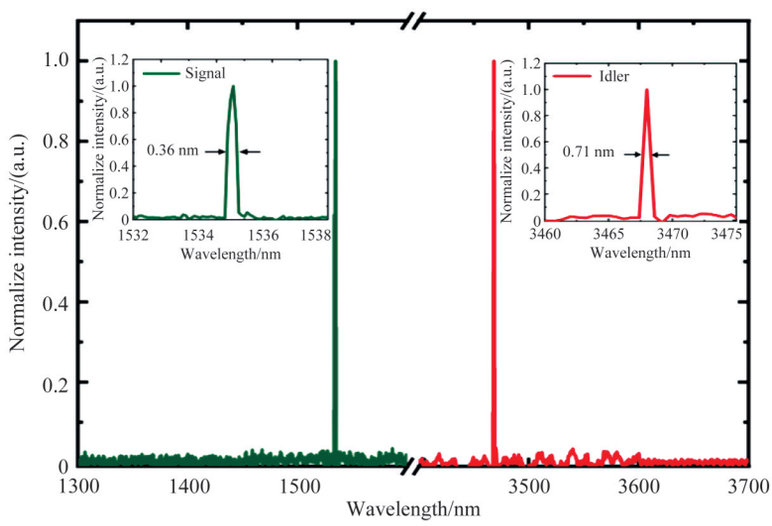

图4 输出信号光(1.535 μm)和闲频光(3.468 μm)的光谱,嵌入图表示输出信号光和闲频光的光谱带宽

Fig.4 Spectrum of the signal and idler outputs at the wavelength of 1.535 μm and 3.468 μm, respectively. Insets show the spectral bandwidth of the signal and idler outputs

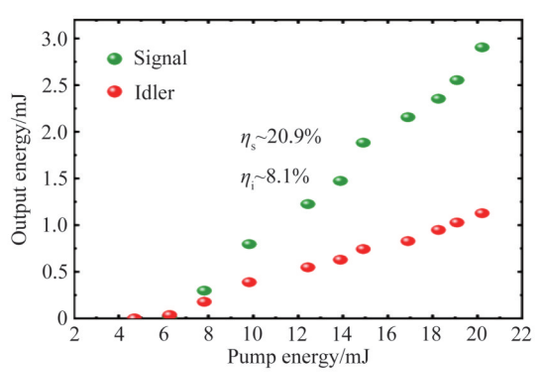

图5 信号光和闲频光输出能量与泵浦光能量之间的函数关系

Fig.5 Signal and idler output energy as a function of the pump energy

3 结论

通过闲频光单谐振KTA-OPO可以得到高光束质量、高能量的近-中红外激光输出。本文由波长为1 μm的纳秒调Q脉冲激光器泵浦一个基于KTA晶体的闲频光单谐振腔得到。通过合理设计腔型、选取高精度参数的谐振腔镜建立了一个稳定紧凑的半球形对称腔,实现了高能量、高光束质量的中红外激光输出。在泵浦光最大的输入能量为20.2 mJ时,输出信号光的最大能量为2.9 mJ、闲频光的最大能量为1.1 mJ,对应的

信号光和闲频光的斜率效率分别为20.9%和8.1%,紧凑稳定的半球形对称闲频光单谐振腔可以有效提高输出激光的能量和转换效率。结合闲频光单谐振光参量振荡器能有效提高输出中红外激光的光束质量特性,测量到输出闲频光在两个正交方向上的光束质量分别为$M_x^2 \approx 1.1$,$M_y^2 \approx 1.1$。高光束质量、高能量的中红外闲频光的产生可以有效促进中红外激光在光谱分析、遥感、痕量气体追踪等多方面的应用。通过合理设计谐振腔型,选取优良光学特性的非线性晶体如MgO:PPLN,可以更近一步拓展高光束质量中红外激光的波段范围,提高中红外激光的输出能量和转换效率。

参考文献

[1] GARBUZOV D, KUDRYASHOV I, DUBINSKII M. 110W (0.9J) pulsed power from resonantly diode-laser-pumped 1.6 μm Er:YAG laser[J]. Applied Physics Letters, 2005, 87(12): 121101.

[2] TAKEI N, SUZUKI S, KANNARI F. 20Hz operation of an eye-safe cascade Raman laser with a Ba $(NO_3)_2$ crystal[J]. Applied Physics B, 2002, 74(6): 521-527.

[3] ASABA K, HOSOKAWA T, HATSUDA Y, et al. Development of 1.54μm near-infrared Q-switched laser [J]. International Society for Optics and Photonics, 1990, 1207: 164-171.

[4] KASKOW M, GORAJEK L, ZENDZIAn W, et al. MW peak power KTP-OPO-based "eye-safe" transmitter[J]. Opto-Electronics Review, 2018, 26(2): 188-193.

[5] DING Xin, FAN Chen, SHENG Quan, et al. 5.2-W high-repetition-rate eye-safe laser at 1525nm generated by Nd: YVO_4-YVO_4 stimulated Raman conversion[J]. Optics Express, 2014, 22(23): 29111-29116.

[6] VAINIO M, HALONEN L. Mid-infrared optical parametric oscillators and frequency combs for molecular spectroscopy [J]. Physical Chemistry Chemical Physics, 2016, 18(6): 4266-4294.

[7] CAI Haoze, BU Lingbing, GONG Yu, et al. Absorption spectrum characteristics of NO_2 near 3.4 μm and its applicationin differential absorption lidar[J]. Acta Photonica Sinica, 2019,48(7): 0701001.
蔡镐泽, 卜令兵, 龚宇, 等. 3.4 μm处NO_2吸收光谱特性及在差分吸收激光雷达中的应用[J]. 光子学报, 2019, 48(7): 0701001.

[8] SIGRIST M W, BARTLOME R, MARINOV D, et al. Trace gas monitoring with infrared laser- based detection schemes [J]. Applied Physics B, 2008, 90(2): 289-300.

[9] DONG Xiaolong, ZHANG Baitao, HE Jingliang, et al. High-power 1.5 and 3.4μm intracavity KTA OPO driven by a diode-pumped Q-switched Nd:YAG laser[J]. Optics Communications, 2009, 282(8): 1668-1670.

[10] DHOLAKIA K, SIMPSON N B, PADGETT M J, et al. Second-harmonic generation and the orbital angular momentum of light[J]. Physical Review A, 1996, 54(5): R3742.

[11] LI Yan, ZHOU Zhiyuan, DING Dongsheng, et al. Sum frequency generation with two orbital angular momentum carrying laser beams[J]. Journal of the Optical Society of America B, 2015, 32(3): 407-411.

[12] XU Lin, CHAN Hoyin, ALAM S U, et al. High-energy, near-and mid-IR picosecond pulses generated by a fiber-MOPA-pumped optical parametric generator and amplifier[J]. Optics Express, 2015, 23(10): 12613-12618.

[13] ABABAIKE M, WANG Shutong, AIERKEN P, et al. Near and mid-infrared optical vortex parametric oscillator based on KTA[J]. Scientific Reports, 2021, 11(1): 1-6.

[14] WARRIER A M, LIN J, PASK H M, et al. Highly efficient picosecond diamond Raman laser at 1240 and 1485nm[J]. Optics Express, 2014, 22(3): 3325-3333.

[15] CHENG L K, CHENG L T, BIERLEIN J D, et al. Properties of doped and undoped crystals of single domain $KTiOAsO_4$[J]. Applied physics letters, 1993, 62(4): 346-348.

[16] SUN Q B, LIU H J, HUANG N, et al. High energy and high efficiency 3.4μm extracavity KTA optical parametric oscillator[J]. Laser Physics Letters, 2011, 8(1): 16-20.

[17] TIIHONEN M, PASISKEVICIUS V, LAURELL F. Spectral and spatial limiting in an idler-resonant PPKTP optical parametric oscillator[J]. Optics Communications, 2005, 250(1-3): 207-211.

[18] NIU Sujian, AIERKEN P, ABABAIKE M, et al. Widely tunable, high-energy, mid-infrared (2.2-4.8μm) laser based on a multi-grating MgO: PPLN optical parametric oscillator[J]. Infrared Physics & Technology, 2020, 104: 103121.

[19] CHEN Bingyan, WANG Yuheng, YU Yongji, et al. Picosecond mid-infrared 3.8μm MgO: PPLN optical parametric oscillator laser with high peak power[J]. Current Optics and Photonics, 2021,5(2): 186-190.

[20] TIIHONEN M, PASISKEVICIUS V, LAURELL F. Spectral and spatial limiting in an idler-resonant PPKTP optical parametric oscillator[J]. Optics Communications, 2005, 250(1-3): 207-211.

[21] BAI Fen, WANG Qingpu, LIU Zhaojun, et al. Idler-resonant optical parametric oscillator based on $KTiOAsO_4$[J]. Applied Physics B, 2013, 112(1): 83-87.

[22] HE Yang, CHEN Fei, YU Deyang, et al. Improved conversion efficiency and beam quality of miniaturized mid-infrared idler-resonant MgO: PPLN optical parametric oscillator pumped by all-fiber laser[J]. Infrared Physics & Technology,

2018, 95: 12-18.
[23] PARSA S, KUMAR S C, NANDY B, et al. Yb-fiber-pumped, high-beam-quality, idler-resonant mid-infrared picosecond optical parametric oscillator[J]. Optics Express, 2019, 27(18): 25436-25444.
[24] NANDY B, KUMAR S C, EBRAHIM-ZADEH M. Yb-fiber-pumped high-average-power picosecond optical parametric oscillator tunable across 1.3-1.5μm[J]. Optics Express, 2022, 30(10):16340-16350.
[25] MENG Jun, LI Chen, CONG Zhenhua, et al. Investigations on beam quality improvement of an NCPM-KTA-based high energy optical parametric oscillator using an unstable resonator with a Gaussian reflectivity mirror[J]. Chinese Optics Letters, 2022, 20(9): 091401.
[26] 买日哈巴·阿巴白克, 王书童, 塔西买提·玉苏甫. 中红外KTA光学参量振荡器的输出特性[J]. 科技与创新, 2021, (12):7-8.

High Energy, High Beam Quality Idler-resonant mid-infrared Optical Parametric Oscillator Based on $KTiOAsO_4$

ZHOU Yuxia, Aiziheerjiang Abulikemu, Dana Jiashaner, Taximaiti Yusufu
(*Xinjiang Key Laboratory for Luminescence Minerals and Optical Functional Materials*, *School of Physics and Electronic Engineering*, *Xinjiang Normal University*, *Urumqi* 830054, *China*)

Abstract: The high energy, high beam quality mid-infrared lasers (3~5 μm), located in the most transparent atmospheric window band, including super-resolution molecular absorption microscopy, molecular spectroscopy, remote sensing, infrared countermeasures, military, and medical treatments, have been widely investigated for a wide variety of applications. In this research, we report on a high energy, high beam quality idler-resonant mid-infrared Optical Parametric Oscillator (OPO) based on a $KTiOAsO_4$ and pumped by a conventional Q-switched Nd:YAG laser. The all solid state Q-switched Nd:YAG laser wavelength at 1.064 μm (25 ns, 50 Hz, and 20 mJ) was used as a pump source, its nearly Gaussian spatial formed output was loosely focused a waist radius of $\omega_0 = 500$ μm to the center of the crystal. A Half-Wave Plate (HWP) and a Thin-Film Polarizer (TFP) were used to control the pump energy injected into the OPO. The idler-resonant oscillator compromised of a concave input mirror (R= 500 mm) with antireflection for pump and high-reflection for signal and idler outputs, and a plane output coupler with partial reflection (R=80%) for idler output, and high transmission to the pump and signal outputs. The physical length of this nearly half-symmetric OPO cavity was fixed ~ 35 mm. The compact half symmetric-stable cavity with appropriate radius curvature of the cavity mirrors provided high efficiency near- and mid-infrared generation. The $KTiOAsO_4$ crystal as a nonlinear parametric gain medium has high transmission in the 3~5 μm region, it was cut along its X-axis (θ=90°, φ=0°) to realize type Ⅱ Noncritical Phase Matching (NCPM) among pump, signal and idler outputs. A Ge filter is used to filter out the signal and undepleted pump beam from the idler output. We recorded the spatial form of pump beam using a conventional CCD camera, a Spiricon pyroelectric camera was also used to observe spatial forms of the signal and idler outputs. With this idler-resonant OPO, we have obtained 2.91 mJ of 1.535 μm near-infrared and 1.13 mJ of 3.468 μm mid-infrared energy outputs at the maximum pump energy of 20.2 mJ, corresponding to the slope efficiencies of 20.9% and 8.1%, respectively. In this system, although the mid infrared idler beam has a large beam divergence, when it is reflected back to the crystal by the input concave mirror with a radius of curvature of 500 mm, it is size reduced to the same size as the pump beam. This greatly increases the spatial overlapping efficiency of the pump and idler fields in a nonlinear crystal, resulting high energy, high beam quality mid-infrared output being achieved in this idler-resonant half symmetric-stable cavity. It is also worth noting that the compared to the signal-resonant OPO with the same pumping and cavity condition, in the idler-resonant OPO, idler beam with large angular dispersion allows to generate narrower spectral bandwidth and higher quality beams, it is an effective approach to improve the beam quality of the mid-infrared output radiation from OPO. We also measured the beam quality factor (M^2) of the mid-infrared idler output by using the knife-edge method, resulting beam quality factors of the idler outputs were $M_x^2 \approx 1.1, M_y^2 \approx 1.1$ along the horizontal and vertical directions, respectively. These values significantly indicated that the idler-resonant OPO can generate excellent beam

quality mid-infrared outputs. We believe that a high energy, high beam quality mid-infrared beam will play an important role in the variety of applications. Further selecting an appropriate nonlinear crystal and optimizing the cavity design are expected to yield improved OPO performance.

Key words: Nonlinear optics; Idler-resonant; Optical parametric oscillator; Beam quality; $KTiOAsO_4$

OCIS Codes: 190.4223; 190.4410; 190.4970

Foundation item: National Natural Science Foundation of China (No. 11664041), Natural Science Foundation of Xinjiang Uygur Autonomous Region of China (No. 2021D01A114), Xinjiang Normal University Key Laboratory of Mineral Luminescent Material and Microstructure of Xinjiang, China (No. KWFG202202)